Polskie Towarzystwo Materiałów Kompozytowych
Polish Society of Composite Materials

25: 4 (2025) 243–251

COMPOSITES THEORY AND PRACTICE

ISSN (online): 2299-128X

Jerzy Morgiel[1, *] (55395998200), Łukasz Maj[1] (0000-0001-8287-0146), Tomasz Suszko[2] (0000-0002-8355-891X), Małgorzata Pomorska[1] (0000-0002-4255-6459), Ewa Dobruchowska[2] (0000-0001-9320-1597), Witold Gulbiński[2] (0000-0001-9771-7451)

[1] *Institute of Metallurgy and Materials Sciences, Polish Academy of Sciences, 25 Reymonta St., 30-059 Kraków*
[2] *Koszalin University of Technology, 2 Śniadeckich St., 75-453 Koszalin*
[*] *Correspondence:* j.morgiel@imim.pl

Received (Otrzymano) 6.10.2025
Published on-line (Opublikowano) 31.12.2025

IN-SITU TEM HEATING OF FENICR/C COATINGS FOR HYDROGEN EVOLUTION REACTION

https://doi.org/10.62753/ctp.2025.02.4.4

The catalytic electrolysis of water enables this process to be performed at low over-potential, and therefore at a lower energy expenditure. Materials like Ni, Mo or W could substitute costly Pt in this role, especially when applied in the form of coatings. Experiments conducted to date have shown that the efficiency of electrolysis is still increasing in the case of metal nano-rods separated by carbon sheets. The present work is aimed at assessing the temperature stability of such a coating obtained by the magnetron sputtering of an AISI 316L (Fe69Cr18Ni11Mo2, in wt%) target in an atmosphere of Ar and C_2H_2. The use of *in-situ* TEM (transmission electron microscopy) heating allowed the start of crystallization of the so-produced coating to be determined, which occurred at ~400°C. Isothermal annealing at this temperature for 1 hour resulted in the predominant precipitation of α-Fe in parallel with a smaller amount of Ni, Fe, C rich nano-particles, while Cr was distributed relatively uniformly throughout the whole coating. Simultaneously, the amorphous carbon underwent transformation to graphite. The experiment showed that the amorphous metal-carbon composite coatings developed for the hydrogen evolution reaction (HER) may be liable to crystallize in the case it was used in the catalytic electrolysis of superheated steam.

Keywords: hydrogen evolution reaction, metal/carbon composites, coatings, in-situ heating

INTRODUCTION

The electrolysis of water is one of main sources of hydrogen, which is planned to substitute petroleum derived fuels. The catalytic properties of platinum electrodes allow the over-potential of this process to be kept at low level, which makes the process energetically viable [1]. However, the high price of noble metals presses researchers to find other solutions.

Transition metals like Ni, Mo, W and especially their carbides might serve as good substitutes for Pt electrodes in electro-catalytic processes, even though their efficiency is only slightly lower [2, 3]. The number of processing steps necessary in the production of solid carbide electrodes turned interest to the physical vapor deposition (PVD) coatings made with carbon. The latter are usually obtained in magnetron stands, but the nickel targets used in such equipment must be alloys with up to ~15 at. % Mo or Cr securing its non-magnetic properties, which guarantees high deposition rates [4–5]. The process is performed in an argon atmosphere with a varying admixture of acetylene or methane allowing the amount of co-deposited carbon to be controlled.

Depending on the chemical composition of the targets and magnetron process parameters, it is possible to obtain either metallic or composite metal/carbon amorphous coatings [5–6]. In the latter case, it is necessary to work with a higher ratio of CH_4 or C_2H_2 in the reactive gas, which results in the development of nano-metallic rods immersed in a carbon matrix.

The heat treatment of metal/carbon amorphous coatings should cause at least their partial crystallization at 450–500°C, i.e. the metallic part should respond in a similar way as it does during the heating of metallic glasses [6, 7]. Their saturation with carbon may, however, slightly shift the transformation temperature toward higher temperatures [8]. The role of amorphous carbon surrounding the metallic components of such composites during heating is less foreseeable because even though it is a fast-diffusing species, the amorphous metallic areas are most probably already oversaturated with it. Simultaneously, the graphitization of amorphous carbon takes place at temperatures in excess of 2500°C. Therefore, the amorphous carbon channels should generally remain in their original form throughout whole applied treatment. Independent of the above problems, after heating such coatings up to ~600°C, one may expect the development of a nano-crystalline metallic/carbon composite microstructure, which has not been yet investigated.

The present experiment was aimed at investigating the crystallization process of magnetron deposited coatings using Fe69Cr18Ni11Mo2 (316L) targets. It was achieved by characterizing their microstructure and phase transitions both in the as-received state and during *in-situ* heating up to ~600°C performed in a transmission electron microscope (TEM). The experiments involved microstructure observations, the acquisition of electron diffractions (ED) as well as scanning transmission electron micrographs backed with X-ray energy dispersive spectroscopy (STEM/EDS) maps presenting local distribution of the alloying elements. All the above was done using thin lamella prepared with the focused ion beam (FIB) technique.

EXPERIMENTAL PROCEDURE

The FeCrNi/a-C:H coatings were obtained by the reactive magnetron sputtering of the AISI 316L alloy (Fe69Cr18Ni11Mo2, in wt%) in an atmosphere of argon and various amounts of acetylene (C_2H_2). Before each deposition process the chamber was evacuated down to ~2×10^{-5} mbar. During deposition, the argon flow was always maintained at 6 sccm, while the C_2H_2 flow was varied from 0 to 4 sccm. Therefore, the total pressure during subsequent processes ranged from 4×10^{-3} to 6×10^{-3} mbar. The unbalanced magnetron electric supply unit working at 1 A and 100 kHz frequency (at 1 kHz modulation) worked with a target 100 mm in diameter. The Si (100) wafers kept at 300°C and under −50 V DC bias potential served as the substrates. According to the ESCA measurements, the above parameters provided up to 44 at. % C in the deposited coating, as described elsewhere [4].

The microstructure of the coatings was characterized with Tecnai G2 and Themis transmission electron microscopes (TEM). The specimens for these experiments were cut both perpendicular and parallel to the surface in the form of ~10 μm x ~6 μm x 100 nm lamella using the Ga^+ focused ion beam (FIB) technique (Fig. 1). The local chemical composition was examined with an integrated X-ray energy dispersive spectroscopy (EDS) attachment. The mappings presenting the distribution of the alloying elements were built of 512 x 512 pixels and acquired with a 1 nm electron probe for 1 hour each. The *in-situ* heating was performed using a single-tilt Gatan 628 heating holder with a tantalum furnace and a 901 hot stage controller. The experiment involved heating the FIB specimens presenting the coatings both in the cross-section and plan-view orientation at 10°C/ min. to the onset of crystallization and holding them at this temperature until the end of amorphous-to-crystalline transformation.

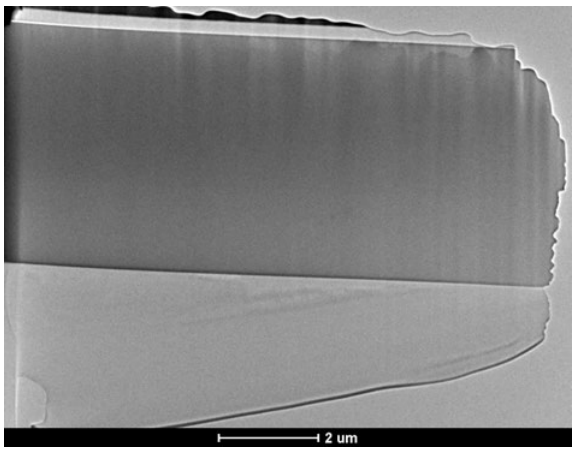

Fig. 1. TEM micrograph of exemplary lamella presenting cross-section microstructure of FeCrNi/a-C:H coating (with objective aperture removed)

RESULTS

The TEM observations performed in BF mode at low magnifications on the lamella cut perpendicularly to the coating surface revealed a lack of any distinct features suggesting its amorphous microstructure (Fig. 2a). Nevertheless, the micrographs acquired using the same mode but at high magnification indicated that the coatings are built of two phases of strongly differing density, i.e. rods of a high average atomic number (Z) separated by thin sheets of low Z matter (Fig. 2b).

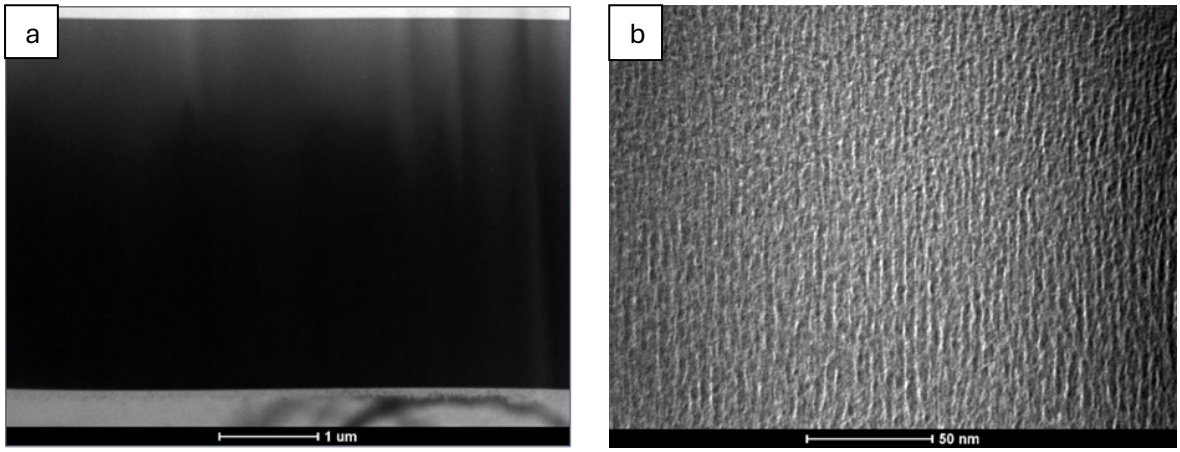

Fig. 2. TEM/ BF low (a) and high magnification (b) micrographs of cross-section of FeCrNi/a-C:H coating

The observations performed using the same approach, but performed on lamella cut parallel to the surface revealed that the high Z nano-rods were indeed fully separated from each other by channels filled with low Z material <1 nm in thickness (Fig. 3). It should be noted that the nano-rods were characterized by a roughly spherical section ~4.5 nm diameter. The electron diffraction patterns acquired from the selected area of this material confirmed the generally amorphous structure of the coatings documented by the presence of two diffused rings at 0.20 nm and 0.12 nm corresponding to nearest neighbors (nn) and next nearest neighbors (nnn), respectively (Fig. 3a, insert). Simultaneously, integrating the intensities along the length of the diffraction vector radii showed that another ring of low intensity was present at ~0.14 nm (Fig. 3c). Dark field images acquired using part of the strongest ring (as marked with a circle in the diffraction pattern) indeed helped to differentiate small bright dots (marked with arrows in Fig. 3b), which represent nano-crystallites or clusters of atoms. The positions of the intensity maxima of the rings on the diffraction pattern points to the possible presence of the α-Fe phase (d_{011} = 0.2027, d_{002} = 0.1433, d_{112} = 0.1170, all in nm).

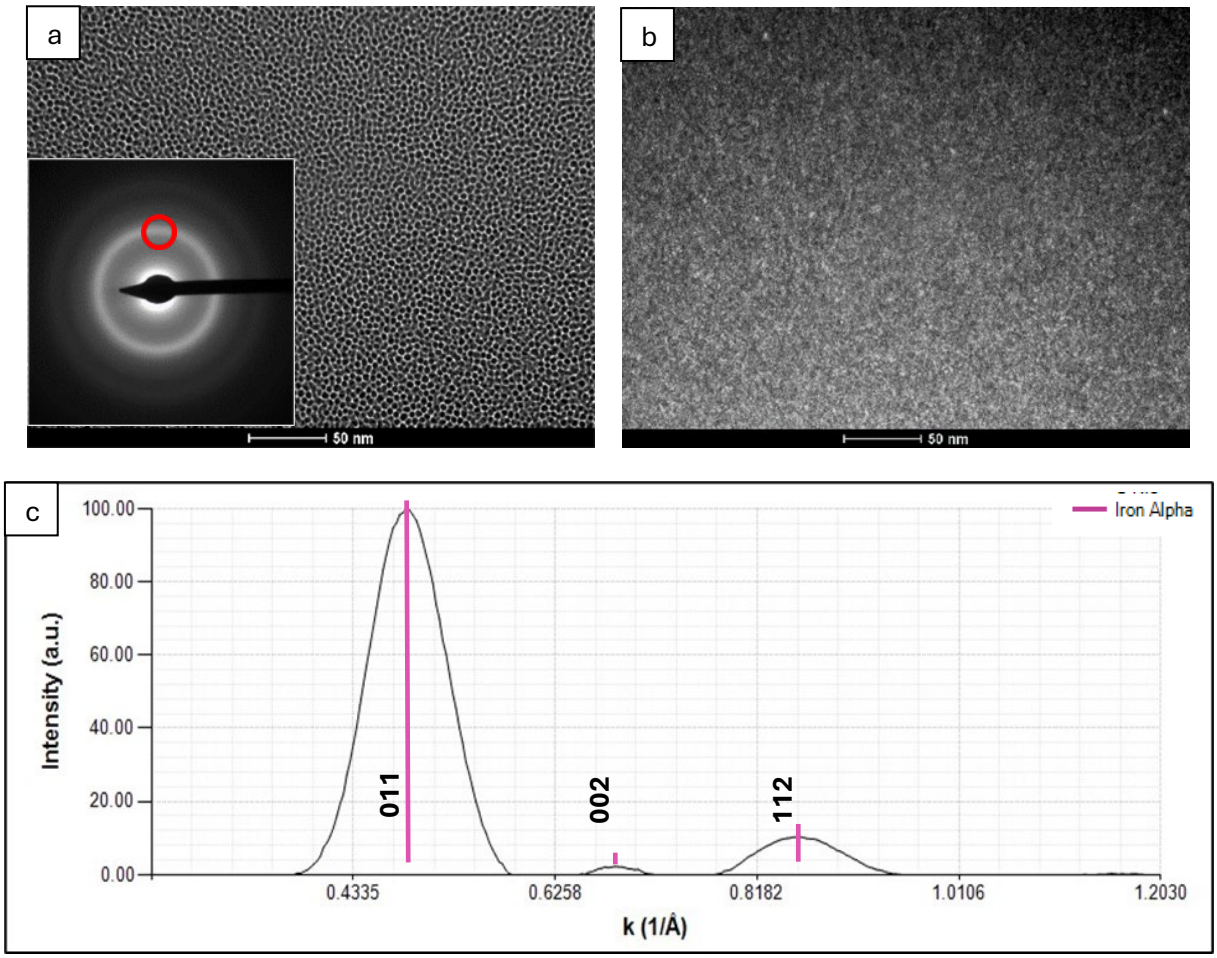

Fig. 3. TEM/ BF high magnification micrograph (a) with selected area diffraction presented as inset and corresponding DF micrograph (b) of parallel-section of FeCrNi/a-C:H coating (red circle on diffraction pattern represents selected area aperture, while nano-crystallites are indicated with arrows), while integrated intensities of diffraction spots are presented in (c)

The *in-situ* TEM heating experiments helped to establish that the first nucleus of the crystalline phase in the investigated FeCrNi/a-C:H coating occurred at ~400°C (Fig. 4a). Continuing heating up to 430°C (Fig. 4b–d) resulted in a fast increase in the density of the crystallites, while above that temperature the number of crystallites in the observed areas remained practically constant (Fig. 4e). It should be noted that the coarsening of crystallites within that time-temperature frame was relatively minor as at the upper temperature range (i.e. 450°C), the size of the nano-crystallites remained roughly the same (Fig. 4e).

Keeping this coating for an extended time at the temperature at which the start of crystallization was observed (i.e. 400°C), resulted in the metallic areas being filled with the crystalline phase (Fig. 5a). The channels separating the crystalline matter remained as a roughly uniform whitish contrast, but a strong difference in the mass thickness contrast between the metallic and carbon dominated phases precluded the determination of the crystallinity of the latter. The dark field (DF) imaging helped to show that even the largest crystallites remained the size of the diameter of the original amorphous metallic columns, though numerous smaller ones were also observed (Fig. 5b). The diffraction of the selected area (placed as an insert in the BF image) showed rings consisting of fine spots from the nano-crystallites. Integrating their intensity along the ring's radii allowed series of partly overlapping peaks to be differentiated, whose positions corresponded to α-Fe, Ni_3C and graphite phases (Fig. 5c).

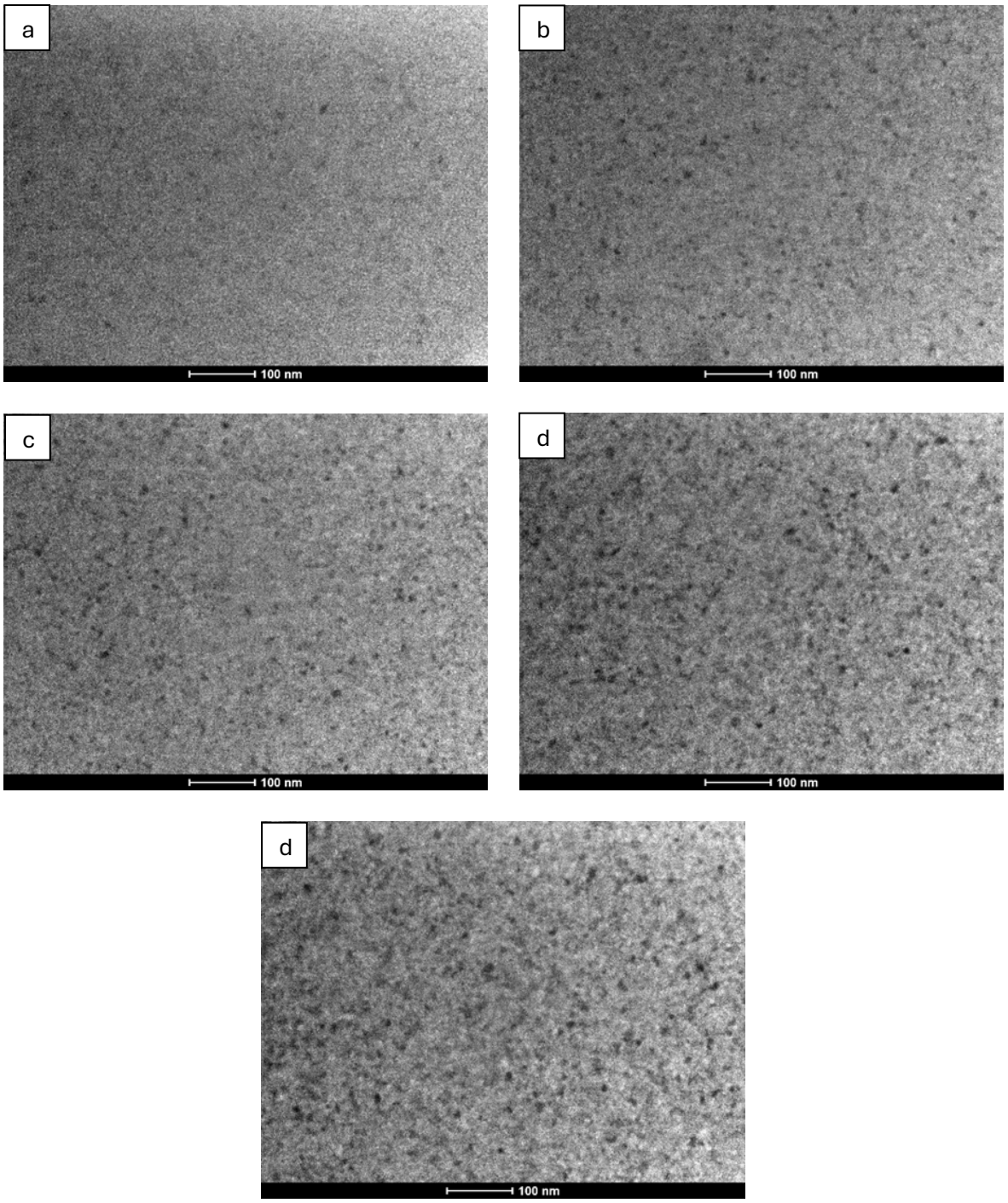

Fig. 4. TEM/ BF high magnification micrographs obtained during in-situ heating of parallel-section of FeCrNi/a-C:H coating at: a) 400°C, b) 410°C, c) 420°C, d) 430°C and e) 450°C

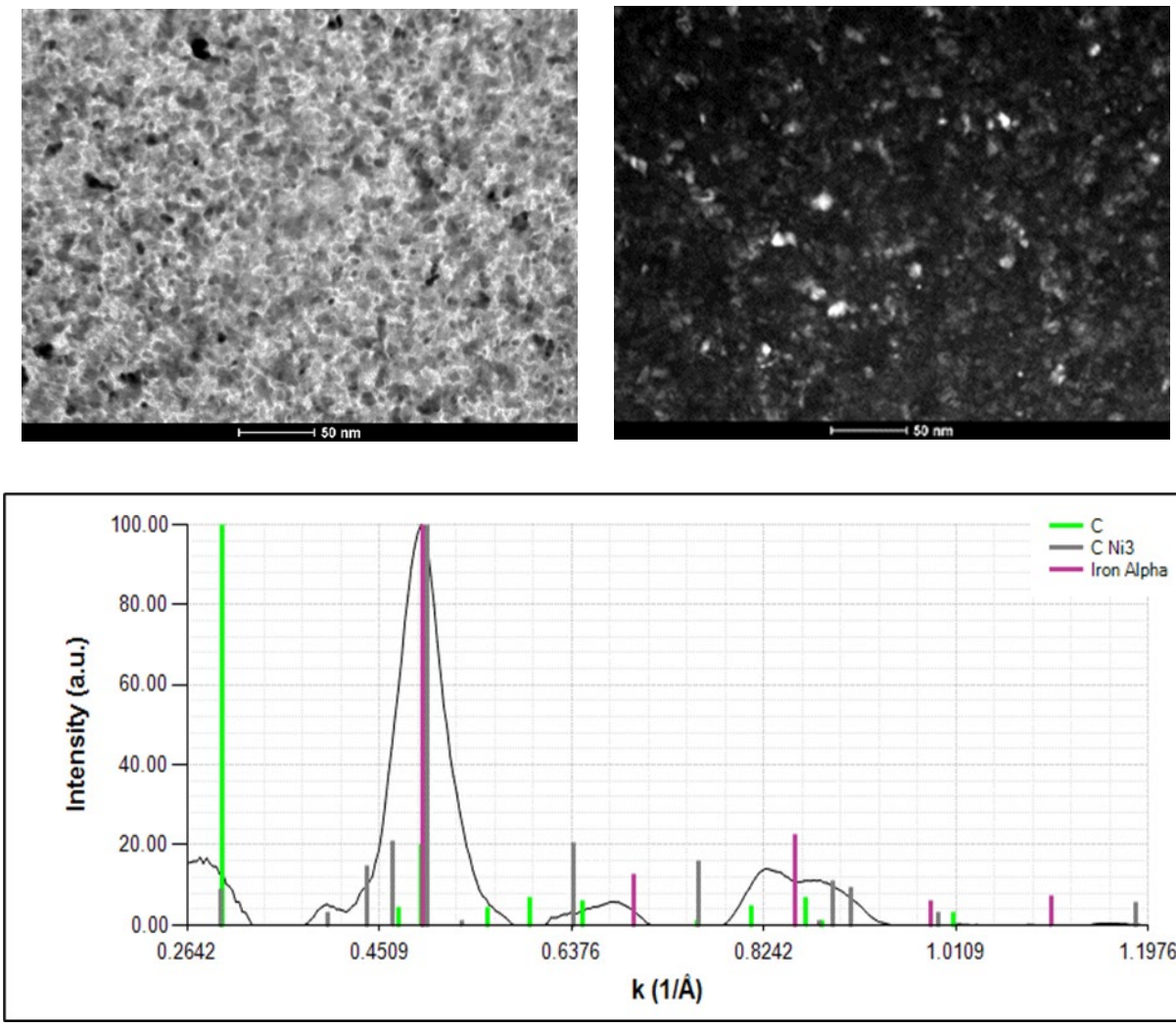

Fig. 5. TEM/ BF (a) and DF (b) high magnification micrographs obtained during in-situ heating of parallel-section of FeCrNi/a-C:H coating at 400°C for 1 h. SA electron diffraction was placed as insert in BF image, while integrated intensities of diffraction spots are presented in (c)

The measurements of the local chemical composition of the coating kept at 400°C for 1 hour performed using the STEM/EDS technique showed the presence of nano-crystalline particles rich either in Ni and Fe or only in Fe, as was documented by maps presenting the distribution of metallic elements as well as the chemical composition profile acquired across a few of them (Fig. 6). The signal from Cr was weak and of a relatively constant intensity throughout the investigated area, indicating uniform distribution of this element. On the other hand, the carbon showed local enrichment among the Fe and (Ni, Fe) rich islands, even though the average level of this element was generally overrepresented due to typical TEM specimen surface contamination with hydrocarbons.

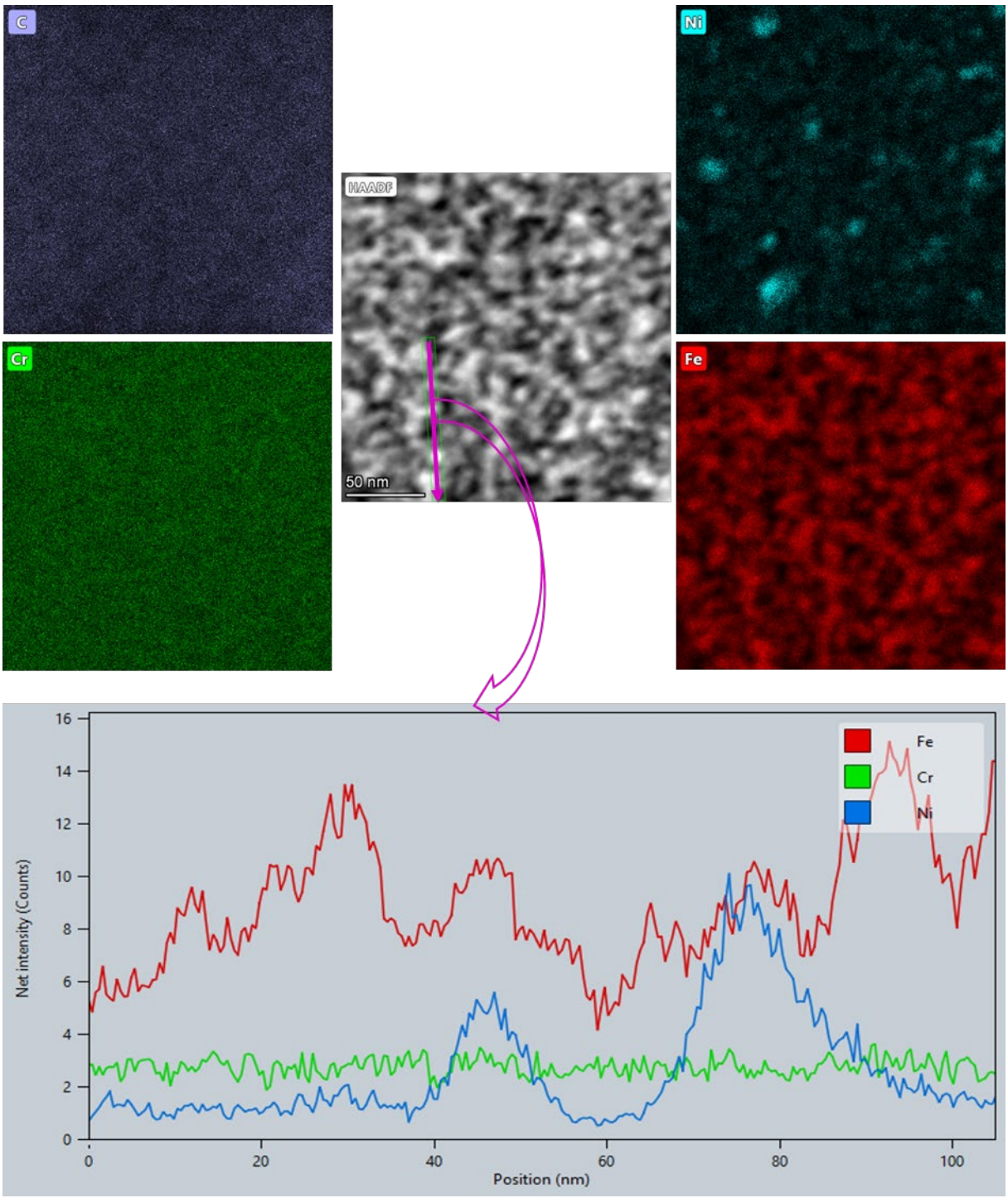

Fig. 6. STEM/ HAADF micrograph obtained during in-situ heating at 400°C for 1 h of parallel-section of FeCrNi/a-C:H coating, accompanied by maps presenting distribution of C, Cr, Fe and Ni, and profile acquired along line marked with arrow

DISCUSSION

The *in-situ* TEM heating at the 10°C/min. rate of the amorphous composite FeCrNi/a-C:H coating showed that its crystallization starts at ~400°C. The relatively slow increase in temperature and approximately uniform distribution of crystallite nucleus in the whole lamella including areas close to its edge, allows us to claim that the observed changes were representative of the *ex-situ* treated material. Literature data concerning experiments with metallic glasses made exclusively of non-ferrous metallic elements like $Ti_{36}Zr_{24}Be_{40}$ [9], $Zr_{62}Al_8Ni_{13}Cu_{17}$ [10] or ZrCuNi [11] located their

crystallization temperature in the 410–460°C range. In the case of iron based metallic glasses, which usually incorporate a significant portion of non-metallic alloying additions, their crystallization temperatures show a much wider scatter, i.e. for the $Fe_{50}Cr_{15}Mo_{14}C_{15}B_6$ alloy it starts at ~370°C [12], for the $Fe_{40}Ni_{40}P_{14}B_6$ alloy at ~400°C [13], while for the $Fe_{72}B_{20}Si_4Nb_4$ alloy it reaches ~570°C [14]. The average chemical composition of the present composite coating, which carried ~44 at. % C (as documented in previous work [4]) locates itself close to the two former of iron based metallic glasses, and, consequently its temperature of the onset of crystallization is one of the lowest for that class of materials.

Electron diffraction helped to establish that annealing at 400°C for 1 hour of the amorphous coating caused its transformation to α-Fe, Ni_3C and graphite. The maps presenting the local chemical composition acquired using the STEM/EDS technique confirmed the nucleation and growth of nano-particles rich in Fe or (Ni, Fe) separated by carbon filled areas. The dominating precipitation of α-Fe was also observed in the case of $Fe_{72}B_{20}Si_4Nb_4$ metallic glass annealed at 550°C for 1 hour, while at higher temperatures such isothermal treatment also caused the nucleation and growth of boride phases (Fe_2B, Fe_3B and $Fe_{23}B_6$) [14], i.e. similar to that produced during the annealing of $Fe_{50}Cr_{15}Mo_{14}C_{15}B_6$ metallic glass [12]. In view of the above, it seems that the precipitation of ferrite is one of the favorable paths during the crystallization of iron based amorphous alloys rich in non-metallic additions, like B or C.

Ascribing a minority fraction of (Ni, Fe) rich particles to Ni_3C carbides precipitating in parallel with α-Fe should be treated as tentative. It is because the differences between Ni_3C and the metastable hexagonal Ni phase unit cell are small and their differentiation with electron diffraction is practically impossible [15]. Additionally, the hex-Ni lattice octahedral interstitial sites are of nearly the same dimensions as those in the austenite in steel, and therefore this phase is capable of accommodating ~10^2 times more carbon than α-Fe. That is why the chemical composition of hex-Ni would be approximately similar to Ni_3C, i.e. beyond the resolution of the EDS system. The transformation of the amorphous carbon channels separating the metallic rich nano-rods in the FeCrNi/a-C:H composite observed in the present experiment may at first seem surprising as usually it requires temperatures in excess of 3000°C and high pressure [16]. Nonetheless, it was already shown by Kono and Sinclair [17] that the thin amorphous layer remaining in contact with the metallic one (Co) changes to polycrystalline graphite at ~500°C. Later on, it occurred that layers of copper [18] or nickel [19] are even more effective in promoting the catalytic graphitization of amorphous carbon.

CONCLUSIONS

The investigations of the microstructure and phase composition of the annealed amorphous FeCrNi/a-C:H composite coating using *in-situ* TEM heating helped to establish that it starts to crystallize already at 400°C. The nano-crystalline products of this transformation consisted predominantly of the α-Fe phase, while the presence of a lesser amount of graphite and nickel-iron-carbon rich particles was also documented. Simultaneously, the chromium addition was observed to be relatively uniformly distributed throughout the heat-treated coating. The performed experiment showed that the amorphous metal-carbon composite coatings developed for HER, like the one deposited in the presented paper, may be liable to crystallize in the case it was used in the catalytic electrolysis of superheated steam.

Acknowledgements

The work was supported by the National Science Centre, Poland within project UMO-2024/53/B/ST11/03015.

REFERENCES

[1] Wang Sh., Lu A. and Zhong Ch-J., Hydrogen production from water electrolysis: role of catalysts, Nano Convergence (2021) 8:4, DOI:10.1186/ s40580-021-00254-x

[2] Amini Horri B. and Ozcan H., Green hydrogen production by water electrolysis: Current status and challenges, Current Opinion in Green and Sustainable Chemistry 2024, 47:100932, DOI:10.1016/ j.cogsc.2024.100932

[3] Idriss H., Hydrogen production from water: past and present, Current Opinion in Chemical Engineering 2020, 29:74–82, DOI: 10.1016/j.coche. 2020.05.009

[4] Suszko T., Gulbiński W., Morgiel J., Greczyński G., Dobruchowska E., Dłuzewski P., Lu J., Hultman L., Amorphous FeCrNi/a-C:H coatings with self-organized nanotubular structure, Scripta Materialia 136 (2017) 24–28, DOI: 10.1016/j.scriptamat.2017.03.040

[5] Suszko T., Nano-columnar, self-organized NiCrC/a-C:H thin films deposited by magnetron sputtering, Applied Surface Science 591 (2022) 153134, DOI: 10.1016/j.apsusc.2022.153134

[6] Suszko T., Dobruchowska E., Gulbiński W., Greczyński G., Morgiel J., Kawczyński B., Załęski K., Dorywalski K., and Pogorzelski S., NiMo-C Coatings Synthesized by Reactive Magnetron Sputtering for Application as a Catalyst for the Hydrogen Evolution Reaction in an Acidic Environment, ACS Appl. Mater. Interfaces 17 (2025) 3344−3355, DOI:10.1021/acsami.4c17743

[7] Jo M.S., Lee J.K., Crystallization behaviour of Zr62Al8Ni13Cu17 Metallic glass, Arch. Metall. Mater. 62 (2017)2B, 1023–1026, DOI: 10.1515/ amm-2017-0146

[8] Wang H-R., Gao Y-L., Hui X-D., Min G-H., Chen Y., Yed Y-F., Effect of Ni content on crystallization of metallic Zr–Cu–Ni glass, Journal of Alloys and Compounds 349 (2003) 129–133, DOI: 10.1016/ S0925-8388(02)00906-4

[9] Nagahama D., Ohkubo T., Hono K., Crystallization of Ti36Zr24Be40 metallic glass, Scripta Materialia 49 (2003) 729–734, DOI: 10.1016/S1359-6462(03) 00337-3

[10] Jo M.S., Lee J.K., Crystallization behaviour of Zr62Al8Ni13Cu17 metallic glass, Arch. Metall. Mater. 62 (2017) 2B, 1023–1026, DOI: 10.1515/ amm-2017-0146

[11] Wang H-R, Gao Y-L., Hui X-D, MinG-H, Chen Y., Ye Y-F., Effect of Ni content on crystallization of metallic Zr–Cu–Ni glass, Journal of Alloys and Compounds 349 (2003) 129–133, DOI: 10.1016/ S0925-8388(02)00906-4

[12] Duarte M.J., Kostka A., Jimenez J.A., Choi P., Klemm J., Crespo D., Raabe D., Renner F.U., Crystallization, phase evolution and corrosion of Fe-based metallic glasses: an atomic-scale structural and chemical characterization study, Acta Materialia 71 (2014) 20–30, doi.org/10.1016/j.actamat. 2014.02.027

[13] Nowosielski R., Babilas R., Structure and properties of selected Fe-based metallic glasses, Journal of Achievements in Materials and Manufacturing Engineering 37 (2009) 332 – 339

[14] He L., Hexagonal close-packed nickel or Ni3C?, Journal of Magnetism and Magnetic Materials 322 (2010) 1991–1993, DOI: 10.1016/j.jmmm.2010. 01.020

[15] Pierson H. O., Handbook of Carbon, Graphite, Diamond, and Fullerenes: Properties, Processing, and Applications, Noyes Publications, New York, 1993, pp. 70–86.

[16] Hou H., Chen Y., Han L., Liu P., Liu Z, Wang Z., Microscopic investigation of Cu-induced crystallization of amorphous carbon at low temperatures, Applied Surface Science 595 (2022) 153507, DOI:10.1016/j.apsusc.2022.153507

[17] Kim J., Son S., Choe M., Lee Z., *In situ* TEM investigation of nickel catalytic graphitization, Materials Today Advances 22 (2024) 100494, DOI:10.1016/j.mtadv. 2024.100494